Effects of elevating temperature and high-temperature annealing upon state-of-the-art of yttia-alumino-silicate fibers doped with Bismuth

D. Ramirez-Granados,[1] A.V. Kir'yanov,[1,3,6] Y.O. Barmenkov,[1] A. Halder,[2] S. Das,[2] A. Dhar,[2] M.C. Paul,[2,7] S.K. Bhadra,[2] S.I. Didenko,[3] V.V. Koltashev,[4] and V.G. Plotnichenko[4,5]

[1]*Centro de Investigaciones en Optica, Loma del Bosque 115, Col. Lomas del Campestre, Leon 37150, Mexico*
[2]*Fiber Optics and Photonic Division, Central Glass & Ceramic Research Institute-CSIR, 196, Raja S.C. Mullick Road, Kolkata-700 032, India*
[3]*National University of Science and Technology (MISIS), Leninsky Avenue 4, Moscow 119049, Russia*
[4]*Fiber Optics Research Center of the Russian Academy of Sciences, Vavilov Street 38, Moscow 119991, Russia*
[5]*Moscow Institute of Physics and Technology, Institutskii per. 9, Dolgoprudny, Moscow Region, 141700, Russia*
[6]*kiryanov@cio.mx*
[7]*paulmukul@hotmail.com*

Abstract: We report an experimental analysis of attenuation and fluorescence (at low-power 750-nm excitation) spectra' transformations in yttria-alumino-silicate fiber doped with Bismuth (Bi), which occur at higher than room, but not exceeding 700°C, temperatures. As well, we address impact of elevating temperature upon the fiber's basic characteristics, such as fluorescence/resonant-absorption saturation, fluorescence lifetime, and pump-light backscattering, given by the presence of Bi-Al related active centers (BACs). The experimental data reveals dramatic impact of heating and high-temperature annealing in excess of 500…550°C on the fiber's state-of-the-art, expressed as significant rise of resonant absorption, enhancement of BACs NIR fluorescence, and reduction of scattering loss. In the meantime, such microscopic parameters of the fiber as BACs fluorescence lifetime and saturation power are found to be kept almost unchanged in its post-annealed state as compared to the pristine one. Possible mechanisms responsible for the phenomena and advantages of utilizing temperature-treated fiber of such type for lasing/amplifying purposes are discussed.

OCIS codes: (060.2290) Fiber materials; (160.2750) Glass and other amorphous materials; (300.6250) Spectroscopy, condensed matter.

References and links

1. E. Dianov, "Bismuth-doped optical fibers: a challenging active medium for near-IR lasers and optical amplifiers," Light Sci. Appl. **1**(5), e12 (2012).
2. E. M. Dianov, "Bi-doped optical fibers: a new active medium for NIR lasers and amplifiers," Proc. SPIE **6890**, 6890H (2008).
3. I. A. Bufetov and E. M. Dianov, "Bi-doped fiber lasers," Laser Phys. Lett. **6**(7), 487–504 (2009).
4. I. Razdobreev, L. Bigot, V. Pureur, A. Favre, G. Bouwmans, and M. Douay, "Efficient all-fiber bismuth-doped laser," Appl. Phys. Lett. **90**(3), 031103 (2007).
5. M. P. Kalita, S. Yoo, and J. Sahu, "Bismuth doped fiber laser and study of unsaturable loss and pump induced absorption in laser performance," Opt. Express **16**(25), 21032–21038 (2008).
6. V. G. Truong, L. Bigot, A. Lerouge, M. Douay, and I. Razdobreev, "Study of thermal stability and luminescence quenching properties of bismuth-doped silicate glasses for fiber laser applications," Appl. Phys. Lett. **92**(4), 041908 (2008).
7. V. V. Dvoyrin, A. V. Kir'yanov, V. M. Mashinsky, O. I. Medvedkov, A. A. Umnikov, A. N. Guryanov, and E. M. Dianov, "Absorption, gain and laser action in bismuth-doped aluminosilicate optical fibers," IEEE J. Quantum Electron. **46**(2), 182–190 (2010).

#251792 Received 12 Oct 2015; revised 27 Nov 2015; accepted 18 Dec 2015; published 15 Jan 2016

8. E. M. Dianov, S. V. Firstov, S. V. Alyshev, K. E. Riumkin, A. V. Shubin, V. F. Khopin, A. N. Gur'yanov, O. I. Medvedkov, and M. A. Mel'kumov, "A new bismuth-doped fibre laser, emitting in the range 1625–1775 nm," Quantum Electron. **44**(6), 503–504 (2014).
9. I. A. Bufetov, M. A. Melkumov, S. V. Firstov, K. E. Riumkin, A. V. Shubin, V. F. Khopin, A. N. Guryanov, and E. M. Dianov, "Bi-doped optical fibers and fiber lasers," IEEE J. Sel. Top. Quantum Electron. **20**(5), 0903815 (2014).
10. S. V. Firstov, V. F. Khopin, I. A. Bufetov, E. G. Firstova, A. N. Guryanov, and E. M. Dianov, "Combined excitation-emission spectroscopy of bismuth active centers in optical fibers," Opt. Express **19**(20), 19551–19561 (2011).
11. V. V. Dvoyrin, V. M. Mashinsky, and E. M. Dianov, "Efficient bismuth-doped fiber lasers," IEEE J. Quantum Electron. **44**(9), 834–840 (2008).
12. D. A. Dvoretskii, I. A. Bufetov, V. V. Vel'miskin, A. S. Zlenko, V. F. Khopin, S. L. Semjonov, A. N. Gur'yanov, L. K. Denisov, and E. M. Dianov, "Optical properties of bismuth-doped silica fibers in the temperature range 300-1500 K," Quantum Electron. **42**(9), 762–769 (2012).
13. I. Razdobreev, H. El Hamzaoui, L. Bigot, V. Arion, G. Bouwmans, A. Le Rouge, and M. Bouazaoui, "Optical properties of Bismuth-doped silica core photonic crystal fiber," Opt. Express **18**(19), 19479–19484 (2010).
14. L. I. Bulatov, V. M. Mashinsky, V. V. Dvorin, E. F. Kustov, E. M. Dianov, and A. P. Sukhorukov, "Structure of absorption and luminescence bands in aluminosilicate optical fibers doped with bismuth," Bull. Russ. Acad, Sci. **72**(12), 1655–1660 (2008).
15. D. A. Dvoretskii, I. A. Bufetov, V. V. Vel'miskin, A. S. Zlenko, V. F. Khopin, S. L. Semjonov, A. N. Gur'yanov, L. K. Denisov, and E. M. Dianov, "Optical properties of the bismuth-doped aluminosilicate fiber within the temperature range 300-1500 K," in Proc. of ICONO/LAT (Moscow, Russia, June 2013), LAT-08 "Fiber Optics" (2013).
16. D. Ramirez-Granados, Y. Barmenkov, A. Kir'yanov, V. Aboites, M. Paul, A. Halder, S. Das, A. Dhar, and S. Bhadra, "The use of yttria-alumino-silicate bismuth doped fibers for temperature sensing," IEEE Photonics J. **7**(4), 6802112 (2015).
17. A. V. Kir'yanov, A. Halder, Y. O. Barmenkov, S. Das, A. Dhar, S. K. Bhadra, V. G. Plotnichenko, V. V. Koltashev, and M. C. Paul, "Distribution of bismuth and bismuth-related centers in core area of Y-Al-SiO_2:Bi fibers," IEEE J. Lightw. Technol. **33**(17), 3649–3659 (2015).
18. M. A. Hughes, T. Suzuki, and Y. Ohishi, "Compositional optimization of bismuth-doped yttria–alumina–silica glass," Opt. Mater. **32**(2), 368–373 (2009).
19. V. O. Sokolov, V. G. Plotnichenko, V. V. Koltashev, and E. M. Dianov, "Centres of broadband near-IR luminescence in bismuth-doped glasses," J. Phys. D Appl. Phys. **42**(9), 095410 (2009).
20. V. O. Sokolov, V. G. Plotnichenko, and E. M. Dianov, "Origin of near-IR luminescence in Bi_2O_3-GeO_2 and Bi_2O_3-SiO_2 glasses: first-principle study," Opt. Mater. Express **5**(1), 163–168 (2015).
21. V. O. Sokolov, V. G. Plotnichenko, and E. M. Dianov, "Interstitial BiO molecule as a broadband IR luminescence centre in bismuth-doped silica glass," Quantum Electron. **41**(12), 1080–1082 (2011).
22. M. Dult, R. S. Kundu, N. Berwal, R. Punia, and N. Kishore, "Manganese modified structural and optical properties of bismuth silicate glasses," J. Mol. Struct. **1089**, 32–37 (2015).
23. B. Xu, S. Zhou, M. Guan, D. Tan, Y. Teng, J. Zhou, Z. Ma, Z. Hong, and J. Qiu, "Unusual luminescence quenching and reviving behavior of Bi-doped germanate glasses," Opt. Express **19**(23), 23436–23443 (2011).
24. G. Lin, D. Tan, F. Luo, D. Chen, Q. Zhao, and J. Qiu, "Linear and nonlinear optical properties of glasses doped with Bi nanoparticles," J. Non-Cryst. Solids **357**(11–13), 2312–2315 (2011).
25. K. H. Nielsen, M. M. Smedskjaer, M. Peng, Y. Yue, and L. Wondraczek, "Surface-luminescence from thermally reduced bismuth-doped sodium aluminosilicate glasses," J. Non-Cryst. Solids **358**(23), 3193–3199 (2012).
26. S. Khonton, S. Morimoto, Y. Arai, and Y. Ohishi, "Redox equilibrium and NIR luminescence of Bi_2O_3–containing glasses," Opt. Mater. **31**(8), 1262–1268 (2009).
27. E. M. Dianov, "Nature of Bi-related near IR active centers in glasses: state of the art and first reliable results," Laser Phys. Lett. **12**(9), 095106 (2015).
28. C. E. Lesher, "Self-diffusion in silicate melts: theory, observations, and applications magmatic systems," Rev. Mineral. Geochem. **72**(1), 269–309 (2010).
29. V. L. Stolyarova, A. L. Shilov, S. I. Lopatin, and S. M. Shugurov, "High-temperature mass spectrometric study and modeling of thermodynamic properties of binary glass-forming systems containing Bi_2O_3.," Rapid Commun. Mass Spectrom. **28**(7), 801–810 (2014).
30. H. W. Guo, X. F. Wang, and D. N. Gao, "Non-isothermal crystallization kinetics and phase transformation of Bi_2O_3-SiO_2 glass-ceramics," Sci. Sin. **43**(3), 353–362 (2011).
31. C.-Y. Wang, G.-Q. Hu, Z.-J. Zhang, B.-Q. Liu, L.-L. Zhu, H. Wang, H.-H. Chen, K. Yang, and J.-T. Zhao, "Preparation and characterization of Bi_2O_3-SiO_2-Al_2O_3 based glasses of good transparency with high Bi_2O_3 content," J. Non-Cryst. Solids **363**(1), 84–88 (2013).
32. K. J. Singh, S. Kaur, and R. S. Kaundal, "Comparative study of gamma ray shielding and some properties of PbO-SiO_2-Al_2O_3 and Bi_2O_3-SiO_2-Al_2O_3 glass systems," Radiat. Phys. Chem. **96**, 153–157 (2014).
33. H. Shim, S. Cho, H. Yie, and H. Kim, "Crystallization behavior of bismuth oxide nano-glass studied via in situ transmission electron microscopy," Ceram. Int. **41**(2), 2196–2201 (2015).
34. M. Peng, C. Zollfrank, and L. Wondraczek, "Origin of broad NIR photoluminescence in bismuthate glass and Bi-doped glasses at room temperature," J. Phys. Condens. Matter **21**(28), 285106 (2009).

#251792 Received 12 Oct 2015; revised 27 Nov 2015; accepted 18 Dec 2015; published 15 Jan 2016

35. Y. Zhao, L. Wondraczek, A. Mermet, M. Peng, Q. Zhang, and J. Qiu, "Homogeneity of bismuth-distribution in bismuth-doped alkali germanate laser glasses towards superbroad fiber amplifiers," Opt. Express **23**(9), 12423–12433 (2015).
36. C. Ban, L. I. Bulatov, V. V. Dvoyrin, V. M. Mashinsky, H. G. Limberger, and E. M. Dianov, "Infrared luminescence enhancement by UV-Irradiation of H2-loaded BiAl-doped fiber," in Proc. of ECOC-2009 (Vienna, Austria, September 2009), 6.1.5 (2009).
37. A. V. Kir'yanov, V. V. Dvoyrin, V. M. Mashinsky, N. N. Il'ichev, N. S. Kozlova, and E. M. Dianov, "Influence of electron irradiation on optical properties of Bismuth doped silica fibers," Opt. Express **19**(7), 6599–6608 (2011).
38. M. Peng, G. Dong, L. Wondraczek, L. Zhang, N. Zhang, and J. Qiu, "Discussion on the origin of NIR emission from Bi-doped materials," J. Non-Cryst. Solids **357**(11–13), 2241–2245 (2011).

1. Introduction

Nowadays, Bismuth (Bi) doped silica fibers (BDFs) attract considerable attention as they exhibit broadband near-infrared (NIR) fluorescence, covering the spectral region that extends from ~1.1 to 1.8 μm, when pumped at wavelengths ranging from ~450 to ~1500 nm, which is an invaluable property for applications in next-day telecom systems. Many compact, versatile, and simple in assembling coherent light sources (lasers and amplifiers) based on BDFs for this, low-loss transmission, window of silica, not matched by any other "active" fibers, have been reported so far. Depending on core-glass chemical composition, BDFs demonstrate diversity of types of fluorescing Bi-related active centers (further – BACs) with a variety of spectral signatures in visible (VIS) and NIR [1–9]. In particular, strong fluorescent ability of BACs, formed in alumino-silicate glasses and fibers and, thus, associated with the presence of Aluminum (Al), is usually observed within the ~1100…1400-nm spectral range at ~1.0…1.1-μm pumping, i.e. at the operation wavelengths of well-developed high-power Ytterbium fiber lasers. However, the nature of BACs responsible for the broadband NIR emission in BDFs, including the ones with alumino-silicate core-glass, is still disputed; moreover, attributing of such-type BACs is controversial. Apparently, absence of clarity of the nature of BACs formed in alumino-silicate fibers and misunderstanding of the mechanisms defining their functionality at pumping into different absorption bands of BACs limit further progress in the area.

A separate point of interest regarding BDFs is impact of heating above room temperature (25°C, further – RT) and pump wavelength's variation upon their absorptive and fluorescent properties; see e.g. Refs [1,4,9–15]. To-date, different kinds of the effect of temperature on basic parameters of BDFs with different core compositions and light sources built on their base have been reported. It also deserves mentioning that BACs NIR fluorescence lifetime, measured in BDFs having different core-glasses and different doping levels, varies from ~0.5 μs to ~1.0 μs at RT [1]. Furthermore, NIR fluorescence of BACs formed in alumino-silicate fibers drops at increasing temperature, the effect known as temperature quenching.

On the other hand, spectral transformations with temperature's variation, adherent to the presence of BACs in alumino-silicate fibers, were poorly addressed in the literature on BDFs. As known to authors, the effect of temperature in such-type BDFs was under scope in very few publications only [9–12,14–16], whilst the results there reported are somewhat contradictory. In virtue of this, the main motivation of the current work was to highlight details of high-temperature-related phenomena in BDFs of such type, *viz*. in yttria-alumino-silicate (YAS) BDFs, for shading more light on the matter. Note that YAS-BDFs is a new material, invented recently [17], although Bi-doped YAS bulk glass was reported earlier [18].

Hereafter, we report the data of an experimental study of thermally-induced changes occurring in the resonant-absorption and NIR fluorescence bands of Bi-Al related BACs at low-power 750-nm excitation in YAS-based BDFs, moderately (see below) doped with Bi, at temperatures ranged from RT to 700°C. These fibers were drawn using a standard drawing tower from nano-engineered YAS-based preforms, obtained through the Modified Chemical Vapor Deposition (MCVD) method employed in conjunction with the Solution-Doping (SD) technique. A comprehensive analysis of the raw preforms and final fibers is provided in [17].

#251792 Received 12 Oct 2015; revised 27 Nov 2015; accepted 18 Dec 2015; published 15 Jan 2016

As follows, we investigate absorption and fluorescence spectra' transformations in these BDFs as well as changes in other basic characteristics of the fibers (fluorescence and resonant-absorption saturation, fluorescence lifetime, pump backscattering at 750-nm excitation, *etc*.), mainly caused by the presence in core-glass of Bi related specie, in function of temperature.

The data reported below were collected at varying temperature between RT and 700°C. It deserves mentioning that, as was checked by means of numerous repetitions of heating/cooling and annealing cycles applied to BDF samples, a trend of partial losing mechanical rigidness (unavoidable at treating any silica fiber at high temperature) becomes detectable in our fibers at temperatures exceeding 680…700°C. Thus, a technical limit of our experiments was chosen to be 700°C.

The results reported in this study reveal a dramatic effect of elevating temperature upon enhancing "state-of-the-art" of the YAS-based BDFs, termed here as significant rise of resonant absorption and NIR fluorescence in the characteristic bands of Bi-Al related BACs during and posterior to high-temperature treatment of the fibers. Possible mechanisms, underlying this – unusual on a first glance – phenomenon, are briefly discussed. It is worth mentioning that, as shown below, in YAS-BDFs annealed at high (over 500…550°C) temperature the changes in the absorption/fluorescence spectra have a non-reversible character, although such microscopic parameters of post-annealed fibers as NIR fluorescence lifetime and fluorescence saturation power are preserved almost unchanged. This fact deserves attention as a valuable property of high-temperature treated BDFs of such or similar [15] type, permitting enhancement of laser/amplifying potential of the fibers. On the contrary, at lower temperatures – ranged from RT to 500…550°C – all found modifications in the BDFs' basic properties are virtually reversible (with no hysteretic behavior observed), allowing, as shown in [16], their use for effective sensing temperature.

We handled in experiments a couple of YAS-based BDFs, both having a relatively high but differing by few-times Bi-doping level, which permits drawing some aspects of the effect of Bi content upon temperature-related phenomena.

2. Fibers characterization and experimental techniques employed

2.1. Fabricating route and basic properties of YAS based BDFs

In experiments were tested the YAS-glass based fibers, labeled hereafter Bi-1 and Bi-2, moderately doped with Bi_2O_3 (~0.6 and ~1.0% wt., respectively) and co-doped with Al_2O_3 (~8.0 wt. %), Y_2O_3 (~2.5 wt. %), and P_2O_3 (in small amount, ~0.2 wt. %). Note that doping levels given here were measured at the preform stage [17] but could be subject to deviations after drawing the fibers (certainly, this applies to Bi content as Bi is known as a very volatile species). Our choice to handle BDFs doped with Bi and Al in a relatively high degree (providing a high concentration of Bi-Al related BACs), was defined by necessity to use short fiber pieces in experiments. In turn, the latter is a requirement of homogeneous heating of fiber samples, ensuring reliability and reproducibility of the collected data.

Doping the fibers with Al_2O_3 solved a few tasks simultaneously: apart from being a pre-requisite for creating Bi-Al related BACs, Al permits engineering of the fiber's numerical aperture (NA) without adding such precursors as Germanium (Ge) and enhances chemical durability of the core-glass, which is important for applications. Adding Y_2O_3 into the core-glass targets facilitating of the radiative transitions between the electronic levels of BACs (phonon energy of Y_2O_3 is one of the lowest cutoffs among oxides [18]) and, eventually, enhances the fluorescent ability of BACs (note that, as compared to [18], doping our fibers with Y_2O_3 was much lower). Adding a small amount of P_2O_5 into the YAS glass aims its softening and accessing phase-separation of nano-sized areas, enriched with Bi [17].

At fabricating Bi doped preforms, un-sintered SiO_2-P_2O_5 soot layers were deposited at 1500 ± 10°C and then soaked in aqueous solution, comprising $Bi(NO_3)_3$, $Al(NO_3)_3$, HNO_3,

#251792 Received 12 Oct 2015; revised 27 Nov 2015; accepted 18 Dec 2015; published 15 Jan 2016

and $Y(NO_3)_3$, for 45 min. This was done using a specially designed SD setup, permitting control over the solution's flow rate at dipping and draining-out stages. The function of P_2O_5 was to achieve nucleation for increasing phase separation besides generation of Bi-rich nano-particles in the core area during porous layers' deposition, while that of HNO_3 was to stop the formation of colloidal $BiONO_3$. Adding Bi into YAS core-glass was fulfilled through SD, followed by suitable thermal treatment. Subsequent to the SD step, dehydration and oxidation of porous layers were made at 900…1000°C. Sintering was conducted gradually by increasing the MCVD burner's temperature from 1500 to 2000°C, followed by collapsing of the tubes. Final fibers were drawn from the preforms using a standard drawing tower.

The major part of the data, presented below (in subsections 3.1 and 3.2), relate to Bi-1 fiber, lower than Bi-2 doped with Bi, since the temperature-induced effects were revealed to be more spectacular in Bi-1 fiber. Meanwhile, we provide (in subsection 3.3) a brief resume of the results obtained with Bi-2 fiber for comparison and, on the other hand, for emphasizing a general character of the temperature-related phenomena in YAS-BDFs.

The three resonant-absorption bands detected in Bi-1 fiber, labelled hereafter I (~750 nm), II (~1000 nm), and III (~500 nm), refer to spectrum 1 in Fig. 1, are the characteristic signatures of BACs, formed in alumino-silicate glasses (YAS glass certainly belongs to this type of glass since Y, at low doping, has the role of a glass modifier). When pumped at 1.06 μm, the fiber demonstrates broadband NIR fluorescence (centered at ~1.15 μm and spanned over ~250…300 nm) and, also, up-conversion emissions (UC) [7], peaked at ~630 and ~750 nm; see spectrum 2 in Fig. 1. The other peaks, at ~1450 and ~860 nm, and the shoulder at the left side of the ~700-nm band of BACs (at ~660 nm) do not relate to Bi doping but, rather (see Ref [17].), stem from the 1st, 2nd and 3rd cutoffs of the fiber, labelled in Fig. 1 as λ_{C1}, λ_{C2}, and λ_{C3}, correspondingly. NA of Bi-1 fiber was measured (at the preform stage) to be ~0.12; so, the fiber demonstrated essentially multimode properties in the spectral range under scope. Note that the ~700-nm and (especially) ~500-nm absorption bands appear on the background that gets elevated towards shorter wavelengths (the well-known fact for Bi-Al related BACs). 1.06-μm pump power, saturating absorption in band II, was estimated to be ~2.5…3 mW.

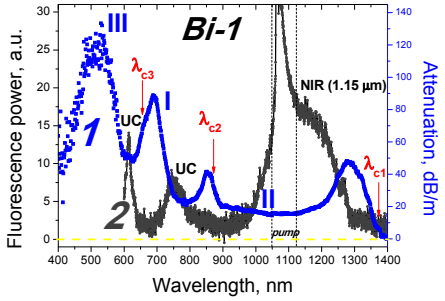

Fig. 1. Spectra of absorption (curve 1) and fluorescence at 1.06 μm pumping (curve 2) of Bi-1 fiber, measured at RT; in both cases short pieces (2…5 cm) of the fiber were under tests. The cutoff features, shown by the vertical red arrows, are addressed in the text.

Bi-2 fiber possesses of very similar to Bi-1 properties, e.g., it has comparable wave-guiding characteristics (say, λ_{C1}~1.5 μm) and almost equal absorption and fluorescence saturation powers. On the other hand, it demonstrates more intensive resonant-absorption bands I to III and stronger NIR fluorescence at both 1.06-μm [17] and 750-nm pumping. But, in overall, the absorption/fluorescence spectra are nearly identical for Bi-1 (see Fig. 1) and Bi-2 fibers. More information about these two BDFs can be found in Ref [17]. where they are referred to as Bi-B and Bi-A, respectively.

#251792 Received 12 Oct 2015; revised 27 Nov 2015; accepted 18 Dec 2015; published 15 Jan 2016

2.2. Experimental equipment and techniques

In all experiments described below lengths of Bi-1 and Bi-2 samples were varied between 1 and 10 cm. The experimental arrangements and equipment are specified as follows.

The experimental setup employed at measurements of the fibers' absorption and NIR fluorescence is sketched in Fig. 2(a). BDF samples were illuminated by a white-light (WL) source (*Yokogawa* AQ4305), at measuring transmission and absorption (after re-calculating measured transmission into absorption, in dB/m) spectra, or were pumped by a 750-nm LED with single-mode fiber output (*Exalos*), at measuring fluorescence spectra. The LED had a rather broad emission spectrum (see Fig. 2(c)) and output power, tunable up to 4.5 mW. It is seen that the LED's operation wavelength matches the right slope of absorption band I of BACs (see Fig. 1). The LED's output was connected to a delivering SMF-28 fiber, spliced with a Bi-doped fiber, the latter placed into an electric oven; its output was spliced with another piece of SMF-28 fiber, connected to either a Ge photo-detector (*Newport*, model 2033, 200-kHz bandwidth), at fluorescence lifetime measurements, or an optical spectrum analyzer (OSA) (*Ando* AQ-6315A), at spectral measurements.

The BDFs' optical transmission spectra were measured employing the cutback method at turning OSA to 2…5-nm resolution. The spectra were recorded before (at RT), at each step of heating and cooling (i.e. at a temperature increase/decrease within the interval RT…700°C), and after completing thermal treatment (normally, after 24 h., which ensured a sample's core-glass relaxation), again at RT. In some of the figures below, the difference spectra – in terms of induced absorption (IA) – are provided, which were obtained after subtraction of the original attenuation spectra of a pristine BDF sample (taken prior to passing it through a heating/cooling cycle) from the ones obtained during or after treating at certain temperature. This allowed a straightforward view on the "net" spectral absorption changes, or IA, within the absorption bands I, II, and III, belonging to Bi-Al related BACs.

At fluorescence lifetime measurements, a NIR fluorescence signal was captured after fast switching pump-light off; the LED's power before pump's blocking was fixed at the maximum (~4.5 mW). To diminish pump background in the measured signal, a long-pass optical filter with cut-on wavelength at ~1000 nm (*Thorlabs*, model FEL1000) was placed between a BDF sample and photo-detector. The resolution of the measurements was ~1.5 μs.

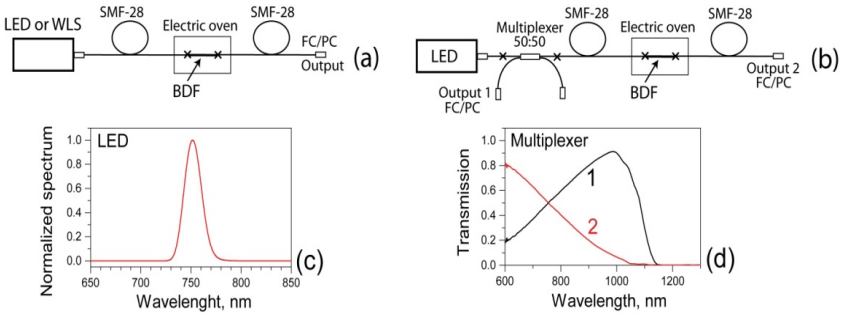

Fig. 2. Experimental arrangements employed at measurements of (a) absorption and fluorescence, including lifetime, and (b) back-fluorescence and backscattering (crosses indicate splices); (c) normalized LED's emission spectrum; (d) multiplexer transmission spectra between the port spliced with SMF-28 fiber (refer to 2(b)) and the port used as output 1 (curve 1) and the port used for connecting with LED (curve 2).

When studying backscattering and backward fluorescence at increasing/decreasing temperature, a fused 50:50 fiber multiplexer for 750 nm was spliced between the LED and first piece of SMF-28 fiber, see Fig. 2(b). In Fig. 2(d), we demonstrate the multiplexer's spectral response in VIS-NIR. Output 1 of the multiplexer was connected with OSA and its unused output was inserted into a cuvette with oil, refractive index of which matches the one of silica (to diminish back-reflection of pump light). The same action and with the same

#251792 Received 12 Oct 2015; revised 27 Nov 2015; accepted 18 Dec 2015; published 15 Jan 2016

purpose was done in these experiments with output of the first SMF-28 fiber. This permitted high-accuracy detection of changes versus temperature in backscattering and backward fluorescence *in situ*.

Regarding the fluorescence measurements, we limited ourselves by collecting the data obtained at exciting BDFs at ~750 nm (the data obtained at moderate-power 1060-nm pumping will be reported elsewhere). Regarding the absorption measurements, we paid most of attention to the changes arising at high temperatures in BACs resonant-absorption bands I and II (these two are most suitable to get lasing), because the ones arising in band III are more complex and need a more comprehensive study.

3. Experimental results and discussion

3.1. Changes in absorptive properties of Bi-1 fiber during and posterior to heating

Here, basic results obtained from the measurements of absorption spectra of Bi-1 fiber during and after treatment at temperatures, ranged from RT to 700°C, are reported.

In main frames of Figs. 3 and 4, we demonstrate, for a 6-cm Bi-1 sample, the temperature dependences of IA in BACs bands I, II, and III (*viz*. in their maxima) during (Fig. 3) and posterior to (Fig. 4) heating/cooling, whilst the overall spectral responses to thermal treatments are exemplified, in either case, in the figures' insets.

Hereafter we denote as ***current temperature T*** the one, measured during a sample's heating (or cooling). In this case, the term IA (***T***) means a current value of additional absorption established in the sample during the process, at ***T***. In turn, we designate hereafter as ***annealing temperature T**** the maximal one, up to which a sample was heated. In this case, the term IA (***T****) applies to additional absorption measured at RT after completing a cycle of heating the sample to ***T****, followed by 1…2-h. annealing, posterior spontaneous cooling down to RT, and thermal relaxation during 24 h.

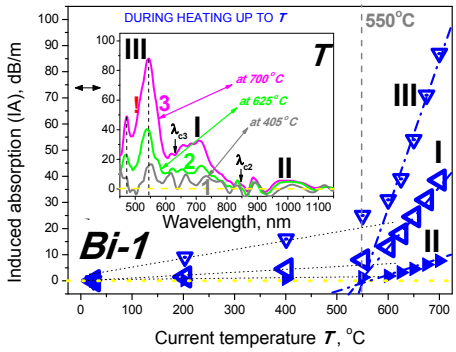

Fig. 3. Dependences of IA establishing in Bi-1 fiber on current temperature ***T*** at heating from RT to 700°C, measured in resonant-absorption bands I, II, and III (represented in main-frame by three blue curves, labelled accordingly). Inset demonstrates the changes in absorption spectra of Bi-1 fiber during heating, "snapshotted" at ***T*** = 405°C (grey curve 1), 625°C (green curve 2), and 700°C (magenta curve 3). Lengths of Bi-1 fiber samples were 6 cm. The dashed and dotted-dashed lines guide to the eye slopes of the dependences as per the presence of the two stages (see text).

It is seen from Fig. 3 that attenuation in all bands monotonously grows with temperature and that two well-definable stages in the process can be segregated: see blue curves in the main frame of Fig. 3. At the first stage (from RT up to 500…550°C), absorption growth in the bands is steep and moderate, whereas at the second one (starting when ***T*** overcomes 550°C and continues up to our limit, 700°C), IA rises with a much bigger slope versus ***T***. An IA-increase at both stages seem to be uncommon, because, as it would be expected, at higher

#251792 Received 12 Oct 2015; revised 27 Nov 2015; accepted 18 Dec 2015; published 15 Jan 2016

temperatures peak absorption ought to decrease (which happens, as we checked using the same experimental arrangement, at heating Erbium doped fibers). Thus, an opposite IA-trend, observed in resonant-absorption bands I, II, and III of Bi-1 fiber at elevating ***T***, is remarkable. Furthermore, the presence of two distinct stages in the process deserves emphasizing as they are probably "switched" by different mechanisms, relating to some transformations happening with BACs and/or their surrounding in the core-glass.

The IA-spectra "snapshotted" at heating Bi-1 sample up to different ***T***, 425°C (curve 1), 605°C (curve 2), and 700°C (curve 3), demonstrate certain deviations from the absorption spectrum of pristine Bi-1 fiber, measured prior to heating (Fig. 1). Some of them are seemingly "imperfections", arising due to the effect of cutoffs (λ_{C2} and λ_{C3}) upon the differential spectra appearance, but others, for instance, a dip within band III, marked as "!" (also reported in [11]), seem to be the features relating to complex nature of BACs formed in YAS-BDFs.

Figure 4 demonstrates another unusual effect observed in Bi-1 fiber, never recorded in earlier studies with BDFs. We plot in this figure the temperature dependences of IA in bands I, II, and III (relative to attenuations in these bands in pristine state of the fiber, i.e. before heating), obtained after turning the fiber to completed cycles of heating to certain temperature ***T**** and posterior cooling to RT.

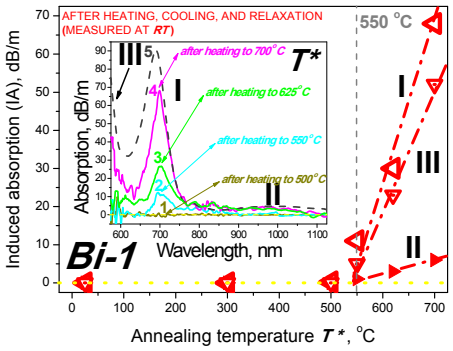

Fig. 4. Dependences of IA established in Bi-1 fiber at RT, as the result of completing cycles of heating/annealing/cooling to RT, on annealing temperature ***T****. As in Fig. 3, in main-frame are shown the data obtained in peaks of resonant-absorption bands I, II, and III (represented by three red curves, labelled accordingly). Inset demonstrates the changes in the resultant (after annealing) absorption spectra of Bi-1 fiber, "snapshotted" at ***T**** = 500°C (olive curve 1), 550°C (blue curve 2), 625°C (green curve 3), and 700°C (magenta curve 4) (measured at RT). Black curve 5 in the inset presents, for comparison, the attenuation spectrum of pristine Bi-1 fiber at RT. Lengths of Bi-1 fiber samples were 6 cm. The dashed and dotted-dashed lines guide to the eye slopes of the dependences as per the presence of the two stages (see text).

On one hand, the result of heating Bi-1 to temperatures not exceeding 500…550°C, no IA is observed to rest after subsequent annealing. That is, the moderate changes in absorption in bands I, II, and III, arising during the first stage of heating up to 550°C (refer to Fig. 3), are reversible. On the other hand, if Bi-1 fiber was heated in excess of 550°C, IA in bands I, II, and III (after cooling and thermal relaxation), strongly increases with ***T****. IA reaches, at maximal ***T**** = 700°C, ~70, ~50, and ~5 dB/m in bands I, III, and II, correspondingly (see the red curves in Fig. 4), i.e. extra-attenuation in these bands becomes comparable with attenuation, measured in pristine state of the fiber. That is, heating of Bi-1 fiber to temperatures higher than 550°C and posterior cooling to RT is an irreversible process, resulted in growth of resonant absorption in the BACs bands twice.

The "frozen" (i.e. taken at RT) IA-spectra, taken after applying whole cycles of heating/cooling, are exemplified in inset to Fig. 4, for a few annealing temperatures: ***T**** =

#251792 Received 12 Oct 2015; revised 27 Nov 2015; accepted 18 Dec 2015; published 15 Jan 2016

500°C (curve 1), 550°C (curve 2), 625°C (curve 3), and 700°C (curve 4). It is seen that annealing at T^* = 500°C does not led to any detectable IA in the fiber's post-annealed state in neither band, whereas at heating to T^* exceeding 550°C the effect of modifying the state-of-the-art of the annealed fiber, in terms of resonant absorption, becomes dramatic. It is also seen from inset to Fig. 4 that rise of attenuation, say, in band I (curve 4) after heating Bi-1 to T^* = 700°C is comparable with the initial attenuation in this band (see curve 5, showing the absorption spectrum of pristine Bi-1 fiber).

The attenuation spectra of a 2-cm Bi-1 sample, obtained for the interval 400…1400 nm and measured at 25°C before thermal treatment (curve 1) and after annealing at T^* = 700°C (curve 2), are demonstrated in Fig. 5(a). Here, again (as in inset to Fig. 4) magenta curve 2 presents the result after applying a complete cycle of the fiber's heating/cooling. The spectra were recorded using a very short Bi-1 sample to enable capturing changes in attenuation (IA) in all resonant-absorption bands, including the one centered at ~500 nm (III), characterized by maximal extinction. The vertical grey arrows in the figure guide to the eye a general trend of increasing attenuation in bands I, II, and III, whereas the vertical red ones designate spectral positions of the cutoff peaks (where, expectedly, almost no changes in attenuation are found as the result of high-temperature treatment).

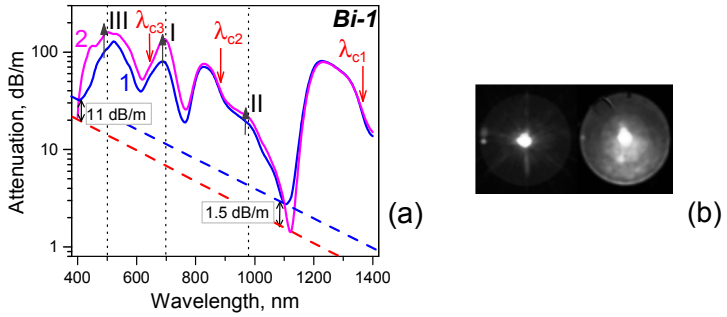

Fig. 5. (a) Dependences of Bi-1 fiber's attenuation, taken in its pristine (before thermal treatment, blue curve 1) and posterior to annealing at T^* = 700°C (i.e. after completing a cycle of heating it to 700°C, followed by annealing, cooling to RT, and thermal relaxing), on annealing temperature T^*. The BACs-related resonant-absorption bands I to III are labelled near the curves. Length of Bi-1 fiber sample tested was 2 cm. The specifications of the features represented by the vertical black / red arrows and by the dashed lines are addressed in the text. (b) Cross-sectional views of Bi-1 fiber (length, 10 cm) cuts, obtained at WL illuminations before (left photo) and after (right photo) completing the whole of thermal treatment: refer to spectra 1 and 2 in main-frame of the figure.

Spectra 1 and 2, when directly compared, allow noticing that the background loss is reduced as the result of high-temperature (in this case, at T^* = 700°C) annealing of Bi-1 fiber. The dashed lines in the figure guide to the eye the feature: it is seen that in NIR the background loss is reduced by ~1.5 dB/m whereas in VIS, say, at ~400 nm, the loss reduction is much bigger, reaching ~11 dB/m.

In Fig. 5(b), we provide the cross-sectional images of Bi-1 fiber, obtained using a microscopy tool of the Vytran equipment under WL illumination before (left side) and after (right side) high-temperature (T^* = 700°C) treatment. In both photos, are seen inner circles, being "replicas" of the over-cladding procedure (made at the fiber's fabrication stage). It is also seen that the fiber's glass takes, after annealing (see the right-side image), some "fogging", mainly produced by WL guidance in core. We can hypothesize that this effect is produced by strengthening of the core-glass inhomogeneity after annealing, probably because of partial crystallization in areas enriched with Bi.

To get more information about the changes in the absorptive properties of Bi-1 fiber during and after heating to a high temperature, a comparative analysis of bands I and II was

#251792 Received 12 Oct 2015; revised 27 Nov 2015; accepted 18 Dec 2015; published 15 Jan 2016

made; see Fig. 6. We exemplify in this figure IA, established in these two bands, when Bi-1 fiber (6-cm in length) was heated to 500°C (a), 550°C (b), 625°C (c), and 700°C (d) (each of the figures was obtained at handling a pristine fiber sample for heating). The blue-color spectra in Fig. 6 were obtained at current (during heating) temperature ***T*** in the oven, whereas the red-color ones – at RT but after completing the cycles of heating/cooling at ***T**** = 500°C, 550°C, 625°C, and 700°C. The black and grey arrows in the panels guide to the eye the spectral widths of bands I and II and the asterisks designate the spectral positions of the artifacts, located in proximity to cutoff λ_{C2} (refer to Figs. 1 and 5(a)).

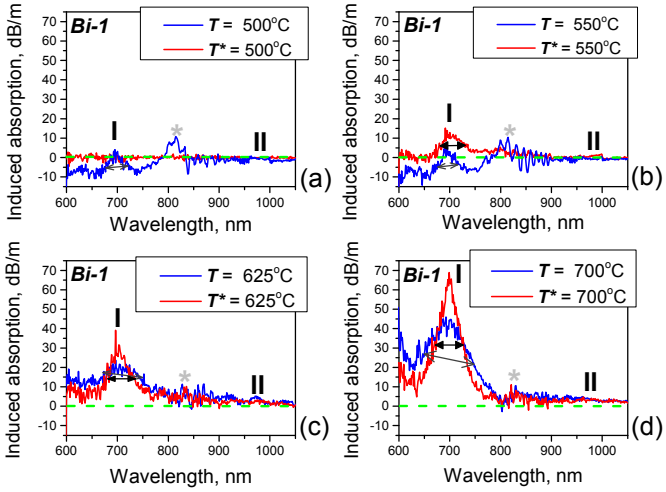

Fig. 6. Examples of IA-spectra measured in the spectral interval, matching resonant-absorption bands I and II, in Bi-1 fibers, obtained at current temperatures at heating (***T***) and after applying cycles of heating/annealing/cooling, *viz*. at annealing temperatures ***T****. The blue and red spectra correspond to different ***T***- and ***T****-values, exemplified by 500°C (a), 550°C (b), 625°C (c), and 700°C (d). Lengths of Bi-1 fiber samples were 6 cm. The black and grey arrows show IA-widths in bands I and II.

A few deserving attention observations can be made from Fig. 6. The first is that in the annealed state of fiber, after passing it through complete cycles of heating/cooling, IA in bands I and II (if presents, which only happens at ***T****>500°C: compare the red spectrum in panel (a) with the red ones in panels (b), (c), and (d)) is substantially bigger than during heating. The second is that, during heating fiber to lower temperatures (exemplified in Fig. 6 by blue spectra, taken at ***T*** = 500°C (a) and 550°C (b)), IA-bands appear on background, or offset, having negative value (with the negativity trend gaining towards shorter wavelengths). This also applies – as our other data show – to lower than 500°C temperatures. The third detail is that in the fiber's heated state IA-bands are always wider than in their post-annealed state: compare the blue and red spectra in all panels of Fig. 6.

The last fact is not surprising, stemming from a common property of resonant-absorption lines widening at elevated temperature; however, the first two ones need a separate consideration. Concerning the second observation, we may propose that the negativity of the offset that the blue spectra in Fig. 6 obey (at lower ***T***) originates from reduction of scattering loss with increasing temperature (a hypothesis in attempt to address this effect is given in subsection 3.2). Regarding the first observation, we think that rise of extinction in the resonant-absorption bands after annealing fiber at temperature higher than ***T**** = 550°C (which is accompanied by rise of NIR fluorescence power of BACs; see subsection 3.2) has another reason. Probably, according to the literature data and to the Raman analysis made in subsection 4.1, its cause is "generating" of extra-BACs (refer again to Figs. 3 and 4) as the result of phase separation/core-glass transformation near/above the transition and

#251792 Received 12 Oct 2015; revised 27 Nov 2015; accepted 18 Dec 2015; published 15 Jan 2016

crystallization temperatures of the core-glass. However, a more detailed study is required in future to accept or reject the hypothesis.

3.2. Changes in fluorescent properties of Bi-1 fiber during and posterior to heating

Here, the fluorescent properties of Bi-1 fiber at low-power excitation at 750 nm in dependence of temperature are presented.

First, we inspected the effect of increasing temperature, from RT up to 700°C, on NIR fluorescence spectra and fluorescence decay transformations, using the setup sketched in Fig. 2(a). Fluorescence in this case was detected at the output of a BDF sample, co-propagating with the rest of pump light (the "forward geometry"). In Figs. 7 to 9 and 12(a) are given the results obtained when 750-nm pump power was fixed at ~4.5 mW, in this experimental configuration. As at measurements of absorption, quite short (2…6 cm) pieces of the fiber were used, which is relevant to high IA-values, established during and after heating (measured by tens of dB/m; refer to Figs. 3 to 6).

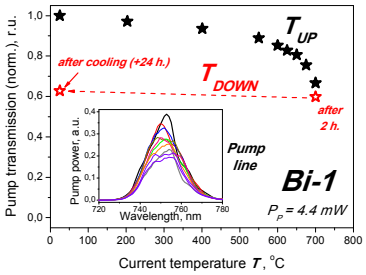

Fig. 7. Normalized dependence of pump-light (750 nm) transmission against temperature $\boldsymbol{T}$ during heating (T_{UP}: black symbols), after 2-h. annealing at $\boldsymbol{T}$ = 700°C (right-hand red symbol), and after annealing, cooling to RT, and thermal relaxation during 24 h. (i.e., $\boldsymbol{T}^*$ = 700°C) (T_{DOWN}: left-hand red symbol). Normalization was done to the transmission of pristine Bi-1 fiber. Pump power at 750 nm, P_P = 4.4 mW, was measured at fiber's input. Inset demonstrates behavior of pump's spectral line in the course of the measurements.

First note that, at increasing temperature from 25°C to 700°C, the remnant LED's power on output of 4-cm Bi-1 fiber steadily decreases; see Fig. 7, where the process is represented by black filled asterisks. This happens because of growth of the fiber's absorption coefficient (IA) at the pump wavelength that matches absorption band I. Transformations in pump-line during heating are demonstrated in inset. The lower than in pristine state (measured at RT) transmission of fiber, reached to the end of annealing at $\boldsymbol{T}$ = 700°C for 2 h. (see the right-hand red open symbol), is partially restored after thermal relaxation (see the left-hand red filled asterisk): the dashed red line in Fig. 7 schematically shows the transience.

[Note that a similar presentation style of the processes, involved during cycles of heating, cooling, and thermal relaxation of Bi-1 fiber, is accepted hereafter (see Figs. 9, 11, and 12), where we report the experimental data on fluorescence and back-scattering. That is, in black color we provide below the data obtained at heating the fiber to certain temperature $\boldsymbol{T}$, whereas in red color – the ones after its annealing at a high temperature (as a rule, at $\boldsymbol{T}^*$ = 700°C), and subsequent leaving it for spontaneous cooling and relaxation (normally, for 24 h.) at RT. The labels $\boldsymbol{T}_{\mathrm{UP}}$ and $\boldsymbol{T}_{\mathrm{DOWN}}$ refer, correspondingly, to the processes of heating and cooling. The data obtained with Bi-2 fiber are presented below by a similar manner; refer to Figs. 17 and 18.]

Elevating temperature resulted in considerable rise of Bi-related NIR (950…1350 nm) fluorescence when Bi-1 fiber was pumped at 750 nm, see Fig. 8. This trend is schematized by the grey vertical arrow in the figure (the different-color spectra in Fig. 8 are labelled by current temperatures at heating, $\boldsymbol{T}$). Note that the fiber's annealing at a high temperature

#251792 Received 12 Oct 2015; revised 27 Nov 2015; accepted 18 Dec 2015; published 15 Jan 2016

(compare e.g. the violet spectra in Fig. 8, obtained at the highest temperature, $\boldsymbol{T}$ = 700°C) led to well-detectable extra-rise of NIR fluorescence. The presence of these phenomena, considered in conjunction with the effect of growing of the resonant-absorption bands at heating (i.e. IA), indicates that high temperature results in increasing content of fluorescing in NIR BACs. Cooling the annealed fiber to RT led to partial "freezing" of NIR fluorescence's rise, arisen during heating/annealing (see the red vertical curve in Fig. 8, showing the trend). This signifies that an increase of concentration of fluorescing in NIR centers, established after passing fiber through a heating/cooling cycle, is non-reversible (hysteretic), which is attractive for applications.

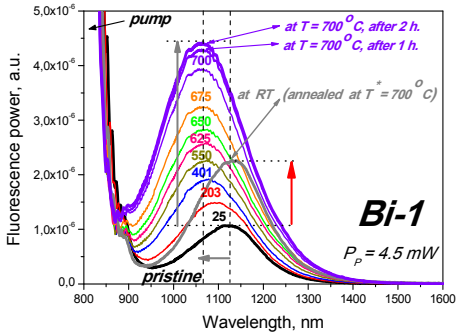

Fig. 8. NIR fluorescence spectra of Bi-1 fiber measured at different temperatures $\boldsymbol{T}$ (labeled near each curve) at heating from RT to 700°C, in "forward geometry". The black spectrum corresponds to pristine state of the fiber while the three violet spectra – to $\boldsymbol{T}$ = 700°C just after establishing this temperature and after 1 and 2 h. of annealing. The grey spectrum, measured at RT, corresponds to the case when Bi-1 sample has passed a whole cycle of heating to 700°C, annealing during 2 h. at this temperature, cooling to RT, and thermal relaxation for 24 h. (i.e. $\boldsymbol{T}$* = 700°C). The arrows guide to the eye the most appreciable trends that NIR fluorescence obeys during thermal treatment. Pump power at 750 nm was fixed at P_P = 4.5 mW.

Another detail seen in Fig. 8 is spectral shifting of the peak of NIR fluorescence, adherent to BACs, to shorter wavelengths with temperature growth; this trend is guided to the eye by the horizontal grey arrow. This feature can be explained by a thermally induced re-distribution between the lower and upper sub-levels of BACs and by weakening, at elevating temperature, of VIS fluorescence centered at ~820 nm (this fluorescence is much less pronounced than NIR one and is almost fading at exceeding $\boldsymbol{T}$ = 550°C; see below).

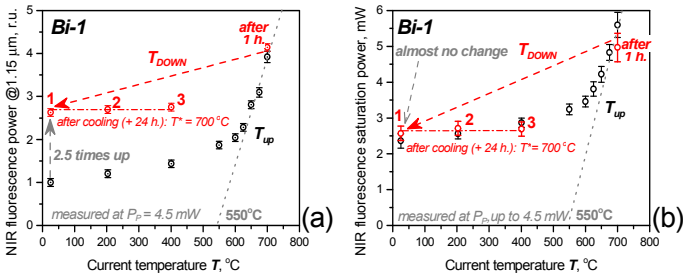

Fig. 9. Dependences of (a) integrated NIR fluorescence power and (b) pump power saturating 1.15-µm fluorescence versus temperature $\boldsymbol{T}$, for Bi-1 fiber. Specified are the processes of heating (T_{UP}: black symbols), 1-h. annealing at $\boldsymbol{T}$ = 700°C (right-hand red symbols), and posterior cooling to RT and thermal relaxation during 24 h. (i.e. $\boldsymbol{T}$* = 700°C) (T_{DOWN}: left-hand red symbols "1"). Red symbols "2" and "3" designate the corresponding parameters' values, measured using the fibers annealed at $\boldsymbol{T}$* = 700°C, re-heated to lower than $\boldsymbol{T}$ = 500°C temperatures. Pump power at 750 nm P_P was varied at measurements of NIR fluorescence saturation (b) from a few µW to 4.5 mW.

#251792 Received 12 Oct 2015; revised 27 Nov 2015; accepted 18 Dec 2015; published 15 Jan 2016

In overall, the dynamics of NIR fluorescence at heating/cooling Bi-1 fiber is demonstrated, as function of ~1150-nm peak's amplitude versus temperature, in Fig. 9(a); these data are complementary to the ones provided in Fig. 8. It is seen that, though rise of NIR fluorescence is monotonous with a ***T*-**increase, two stages with considerably different slopes of NIR power versus ***T*** can be segregated: the first at ***T*** changing from RT to 550°C and the second at ***T***>550°C (the latter is fitted by the grey dotted line). It deserves attention that, at maximal temperature (***T*** = 700°C), growth of NIR fluorescence power bigger than 4X is reached. The presence of the two stages in NIR fluorescence's growth is complementary to what is observed regarding IA in resonant-absorption bands I to III (refer to Fig. 3). Interestingly, if the sample's temperature did not exceed ***T***~550°C at heating, the changes in NIR fluorescence power after cooling (at ***T****<550°C) were reversible. In other words, no hysteresis in fluorescent ability of the annealed fiber was observed. In contrast, at heating the sample up to ***T***>550°C, NIR fluorescence at the end of a heating/cooling cycle was "frozen" at a ~2.5 higher level as compared to its pristine state. The effect is marked by point "1" and by the vertical arrow in Fig. 9(a). Thus, a hysteretic behavior of NIR fluorescence complements the IA-behavior (also hysteretic) in resonant-absorption bands I to III (refer to Fig. 4).

Note that posterior, or "secondary", heating of heat-treated fibers up to ***T*** (a few experiments of such type were conducted at annealing Bi-1 fiber at ***T**** = 700°C) did not lead to detectable change of NIR fluorescence (see points "2" and "3" in Fig. 9(a), specifying the said).

In Fig. 9(b), are shown the results of measurements of pump power at ~750 nm saturating NIR fluorescence (P_P^{sat}); these data were obtained after proceeding the NIR fluorescence spectra (see Fig. 8), recorded at varying P_P from small-signal (tens μW) to maximal (4.5 mW) values, for each ***T***, during heating/cooling cycles. For a pristine sample, P_P^{sat} is measured by ~2.5 mW, while at heating it up to 700°C P_P^{sat} increases up to 5.0…5.5 mW but restores, after thermal relaxation, down to the initial value (~2.5 mW). Furthermore, similarly to the results presented in Fig. 9(a), two stages in P_P^{sat}-growth, at ***T***<550°C and at ***T***>550°C, can be segregated, with slope of the process at the second stage being considerably bigger.

As it happens with NIR fluorescence power (refer to Fig. 9(a)), posterior heating of annealed Bi-1 fibers up to ***T*** higher than RT but lower than 550°C (see points "1", "2", and "3" in Fig. 9(b)) does not result in any change in P_P^{sat}. Thus, the overall result of applying cycles of heating/cooling is always reversible, in contrast to the trend obeyed by NIR fluorescence against ***T*** (compare the data marked as "1", "2" and "3" in Figs. 9(a) and 9(b)).

A piece of further information about the heating effect on the fluorescent properties of Bi-1/Bi-2 fibers was revealed from the measurements in "backward geometry" (see the setup shown in Fig. 2(b)). The results of measuring the emission spectra, comprising back-fluorescence of BACs and pump-light backscattering, are demonstrated in Figs. 10 and 11 for Bi-1 fiber (we used in these experiments 8-cm samples of the fiber).

The experiments were conducted at maximal pump power, which however was lowered by approximately two times, down to P_P~2.1 mW, in the 50:50 multiplexer, used for measuring back-fluorescence (see Fig. 2(b)). Note that the multiplexer had suitable spectral transmission between 700 and 1100 nm (Fig. 2(d)), enabling measuring back-fluorescence in both contributing BACs bands, NIR (centered at 1.15 μm, refer to Fig. 9) and VIS (centered at 820 nm), and 750-nm pump backscattering.

#251792 Received 12 Oct 2015; revised 27 Nov 2015; accepted 18 Dec 2015; published 15 Jan 2016

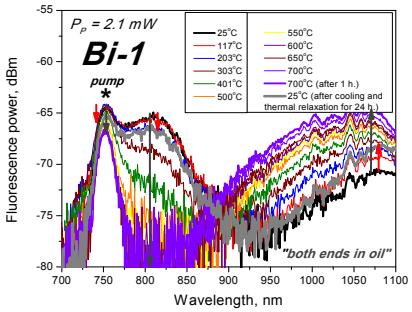

Fig. 10. VIS to NIR fluorescence spectra of Bi-1 fiber measured at different temperatures ***T*** (their values are provided in the legend in top-right corner) at heating from RT to 700°C, in "backward geometry". The black spectrum corresponds to pristine state of the fiber while the two violet curves demonstrate the spectra obtained at ***T*** = 700°C just after establishing this temperature and after 1 h. of annealing. The grey spectrum, measured at RT, corresponds to the case when Bi-1 sample has passed a whole cycle of heating to 700°C, annealing during 1 h. at this temperature, cooling to RT, and thermal relaxation for 24 h. (i.e. ***T**** = 700°C). The arrows guide to the eye the most appreciable trends that VIS and NIR fluorescence obeys during thermal treatment. Pump power at 750 nm (its spectral component is asterisked in the figure) was fixed at P_P = 2.1 mW.

As seen from Fig. 10, the NIR fluorescence (centered at 1.15 μm) demonstrates rise, by more than 11 dB, during heating (which is marked by the vertical grey arrow, at the right side of the figure). In turn, its enhancement to the end of the heating/cooling cycle, by more than 2.5 dB, should be noticed (the effect is sketched by the red arrow at the right side of Fig. 10). This result is similar to what was found at spectral measurements in "forward geometry": refer to Fig. 8 and the discussion therein. On the contrary, both VIS fluorescence, centered at 820 nm, and pump-scattering component at 750 nm (asterisked) are seen to drop at heating, with the former vanishing at ***T***>550°C (see the vertical grey arrows at the left side of the figure, clarifying the feature). Furthermore (on the contrary to what happens with NIR fluorescence), both VIS fluorescence and pump backscattering restore, but partially, at the end of the heating/cooling cycle, which is schematized by the red arrows at the left side of Fig. 10.

The overall "dynamics" of the last two effects during heating/cooling is presented in Fig. 11 for Bi-1 fiber, where backscattering of pump-light component (asterisked in Fig. 10) and VIS back-fluorescence (in maximum, at 820 nm) are plotted versus ***T***; see panels (a) and (b), respectively.

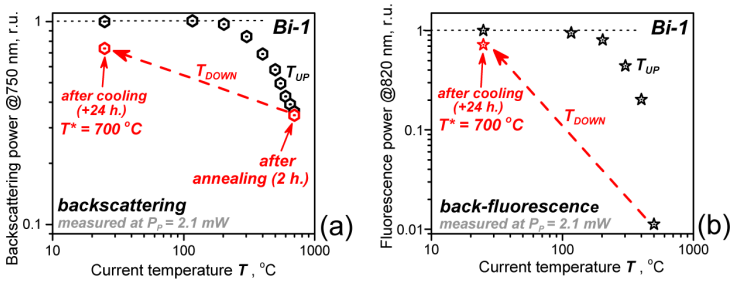

Fig. 11. Normalized dependences of (a) backscattering at pump wavelength (750 nm) and (b) VIS back-fluorescence (centered at 820 nm) powers against temperature ***T*** during heating (T_{UP}: black symbols), after 2-h. annealing at ***T*** = 700°C (right-hand red symbols), and after annealing, cooling to RT, and thermal relaxation during 24 h. (i.e. ***T**** = 700°C) (T_{DOWN}: left-hand red symbols). Normalization was done to the plotted parameters' values measured using pristine Bi-1 samples; pump power at 750 nm was kept at P_P = 2.1 mW.

#251792 Received 12 Oct 2015; revised 27 Nov 2015; accepted 18 Dec 2015; published 15 Jan 2016

The demonstrated dependences allow one to compare the laws obeyed by the two quantities, already discussed at analyzing Fig. 10 (also compare these with the "dynamics" of NIR fluorescence, presented in Fig. 9(a)). It is seen from Fig. 11 that both pump scattering and 820-nm fluorescence strongly fade at heating but partially restore after cooling the fiber, whereas NIR fluorescence (at ~1.15 μm; refer again to Figs. 8 and 10) takes an opposite trend: it rises at heating but partially fades at cooling. This means that the "objects" responsible for the phenomena are different, being probably different Bi related centers. Moreover, given that pump-scattering ought to be produced by rather large objects, such as nano-sized Bi-clusters, and that pump scattering and 820-nm fluorescence demonstrate similar dynamics versus $\boldsymbol{T}$ (see Fig. 11), such clusters seem to be as well responsible for VIS (820-nm) fluorescence. The processes involved at heating/cooling Bi-1 fiber can be, for example, local melting/solidification of Bi-clusters. On the other hand, since NIR (1.15-μm) fluorescence has the opposite trend at heating/cooling (see Fig. 9), the objects producing it may be simpler organized Bi-related centers, generated under heating and preserved in part after annealing.

Figure 12 demonstrates the results of measurements of (a) NIR (centered at 1.15 μm) and (b) VIS (centered at 820 nm) fluorescence lifetimes, τ_1 and τ_2, against temperature $\boldsymbol{T}$ during heating ($\boldsymbol{T}_{UP}$) and after applying a cycle of heating/cooling ($\boldsymbol{T}_{DOWN}$), in Bi-1 fiber. In the first case, the measurements were performed in "forward geometry" (refer to Fig. 2(a)) and in the second one – in "backward geometry" (refer to Fig. 2(b)). We used at these measurements Bi-1 samples 4 and 8 cm in length, respectively.

It is seen from Fig. 12 that both lifetimes decrease with temperature ($\boldsymbol{T}_{UP}$) and that the effect is stronger in case of 820-nm fluorescence. It is also seen (compare the black symbols forming curves 1 and 2) that, whereas 1150-nm fluorescence lifetime (τ_1) decreases at the highest accessible temperature $\boldsymbol{T}$ = 700°C by ~25% as compared to its value (~800 μs) measured before heating, 820-nm fluorescence lifetime (τ_2) drops at $\boldsymbol{T}$ exceeding 500°C by an order of its initial value (~10 μs). [Note that at $\boldsymbol{T}$>500°C the temporal resolution of our experimental setup did not permit reliable measurements.] It deserves attention, regarding 820-nm fluorescence, that (see also Fig. 10) it vanishes at $\boldsymbol{T}$~550°C, which, seemingly, is the result of not only τ_2-drop with $\boldsymbol{T}$ but also of a decrease of content of Bi related centers, emitting at 820 nm. Apparently, these centers are not BACs, responsible for 1.15-μm fluorescence, as concentration of these is supposed to increase at heating (refer to the spectra shown in Fig. 10).

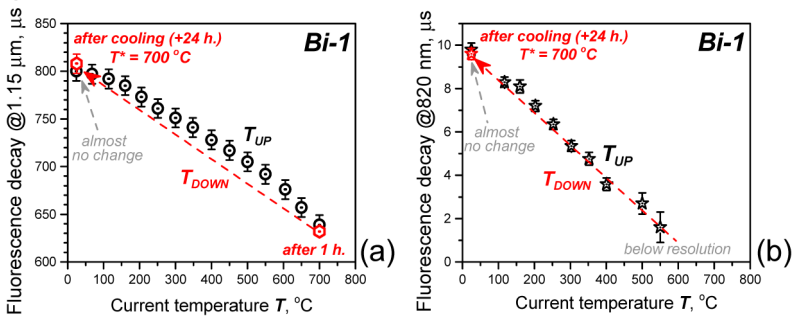

Fig. 12. Dependences of (a) NIR (centered at 1.15 μm) and (b) VIS (centered at 820 nm) fluorescence lifetimes against temperature $\boldsymbol{T}$ during heating (T_{UP}: black symbols), after 1-h. annealing at $\boldsymbol{T}$ = 700°C (right-hand red symbols), and after annealing, cooling to RT, and thermal relaxation during 24 h. (i.e. $\boldsymbol{T}^*$ = 700°C) (T_{DOWN}: left-hand red symbols).

It is worth mentioning that spontaneous cooling of Bi-1 fiber to RT (see the red arrows in the figure, attributing this process as $\boldsymbol{T}_{DOWN}$), both lifetimes, τ_1 and τ_2, "return" (within the experimental errors) to the values, measured prior to thermal treatment. This leads to a

#251792 Received 12 Oct 2015; revised 27 Nov 2015; accepted 18 Dec 2015; published 15 Jan 2016

reversible (non-hysteretic) character of the changes that both lifetimes suffer at increasing/decreasing temperature, *viz*. insignificance of the fiber's annealing at any ***T**** upon its final state. This is not surprising because fluorescence lifetime is a microscopic parameter, inherent to an emitting object (in our case, BACs), but is irrelevant to the objects' overall content, subjected to changes, seen as rise of resonant absorption in bands I to III and rise of NIR fluorescence. The same logics certainly applies to fluorescence saturation power (see Fig. 9(b)), which is as well a microscopic parameter, attributed by inherent properties of BACs, not by BACs concentration.

The revealed character of fluorescence at high temperatures was repeatedly confirmed in our experiments at handling Bi-1 samples of different lengths, which ensures that a true effect of NIR fluorescence enhancement exists. Furthermore, similar in appearance but weaker changes in BACs fluorescence were detected in Bi-2 fiber (see subsection 3.3). On the other hand, note that the data, recently published for another type of alumino-silicate BDF (free from Y co-doping while much lighter doped with Bi) [15], showed a similar trend of NIR fluorescence at annealing, while at much higher (~1200°C) temperatures.

3.3. Effect of temperature upon absorptive and fluorescent properties of Bi-2 fiber

Here we present some data on the absorptive and fluorescent properties of Bi-2 fiber, ~3-times heavier doped with BACs than Bi-1 fiber, in function of temperature. These experiments were made using the same equipment and employing the same setups sketched in Fig. 2 but at handling shorter pieces of Bi-2 fiber, given that its absorption in the resonant-absorption bands is higher. The aim is, on one hand, to demonstrate similarity of this and Bi-1 fiber in susceptibility to thermally induced effects, whilst, on the other hand, to draw differences between them, regarding the effect of high temperatures. We do not consider here in full the data collected with Bi-2 fiber, but, rather, present a brief resume of the featuring results.

In Fig. 13 (analogous to Fig. 6 where the data for Bi-1 fiber are provided), we exemplify IA-spectra in absorption bands I and II, produced in 2-cm Bi-2 fiber samples at heating them up to 550°C (a) and 700°C (b). As in Fig. 6, the blue-color spectra correspond to current (during heating) temperatures ***T***, whereas the red-color ones – to annealing temperatures ***T****; again the arrows in two panels of Fig. 13 guide to the eye spectral widths of bands I and II.

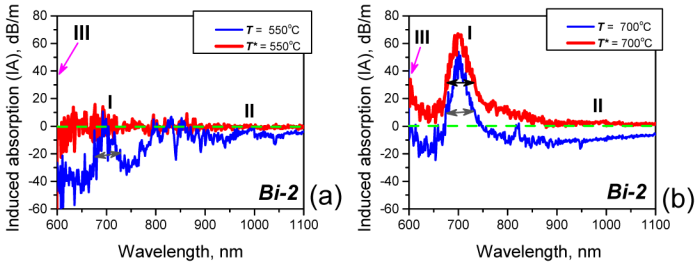

Fig. 13. Examples of IA-spectra measured in the spectral interval, matching resonant-absorption bands I and II, in Bi-2 fibers, obtained at current temperatures at heating (***T***) and after applying cycles of heating/annealing/cooling, *viz*. at annealing temperatures ***T****. The blue and red spectra correspond to ***T***- and ***T****-values, exemplified by 550°C (a) and 700°C (b). Lengths of Bi-2 fiber samples were 2 cm. The black and grey arrows show IA-widths in bands I and II.

It is seen that in the annealed state of Bi-2 fiber IA in bands I and II (at ***T****>550°C) is much bigger than IA during heating (compare the red and blue spectra in Fig. 13) and that the spectra recorded during heating (the blue ones) are "offset" over background, demonstrating a negativity trend gaining towards shorter wavelengths, similarly to what happens with Bi-1 fiber. However, in difference to Bi-1 fiber, the last feature (argued above to relate to a decrease of scattering-loss in the fiber at heating) is essential in Bi-2 even at the highest (***T*** =

#251792 Received 12 Oct 2015; revised 27 Nov 2015; accepted 18 Dec 2015; published 15 Jan 2016

700°C) temperature; see Fig. 13(b) and compare it with Fig. 6(d). Furthermore, the effect of IA-rise in the resonant-absorption bands of BACs after annealing at higher than T^* = 550°C is as well notable in Bi-2 fiber (compare the red spectra in panels (a) and (b) of Fig. 13). However, ratio of IA to the absorption peak value (A_{PR}) in the resonant bands of pristine fiber, i.e. IA/A_{PR}, is smaller in case of Bi-2 fiber (~0.2…0.25) than in case of Bi-1 (>0.5) one.

In Fig. 14 (analogous to Fig. 4, reported for Bi-1 fiber), we demonstrate, for Bi-2 fiber, the dependences of IA in resonant-absorption bands I to III (see the red curves in main frame, accordingly labeled) on annealing temperature T^*. In inset to the figure, the IA-spectra (see curves 1 to 4), recorded at T^* = 500°C, 550°C, 625°C, and 700°C are "snapshotted" for getting more details about the phenomenon, whilst curve 5 shows, for comparison, the absorption spectrum of pristine Bi-2 fiber.

From Fig. 14, it is seen that IA grows drastically, in each band, after passing the temperature "threshold", T^* = 550°C, similarly to what was revealed for Bi-1 fiber (refer to Fig. 4). However, maximal IA-values accessible at T^* = 700°C in case of Bi-2 fiber, although comparable in absolute values with those for Bi-1 fiber, are – in terms of IA/A_{PR} – less, not exceeding 0.2…0.25.

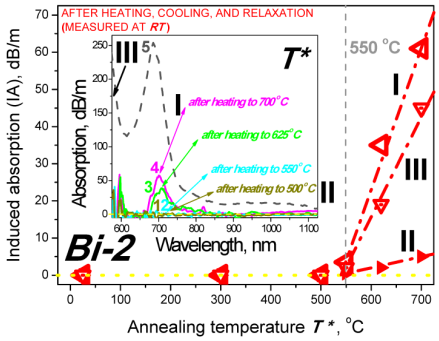

Fig. 14. Dependences of IA established in Bi-2 fiber, as the result of completing cycles of heating/annealing/cooling to RT, on annealing temperature T^*. In main-frame are shown the data obtained in peaks of resonant-absorption bands I, II, and III (represented by the three red curves, labelled accordingly). Inset demonstrates the changes in the resultant (after annealing) absorption spectra of Bi-2 fiber, "snapshotted" at T^* = 500°C (olive curve 1), 550°C (blue curve 2), 625°C (green curve 3), and 700°C (magenta curve 4) (measured at RT). Black curve 5 presents, for comparison, the attenuation spectrum of pristine Bi-2 fiber. Lengths of Bi-2 fiber samples were 2 cm. The dashed and dotted-dashed lines guide to the eye slopes of the dependences as per the presence of the two stages (see text).

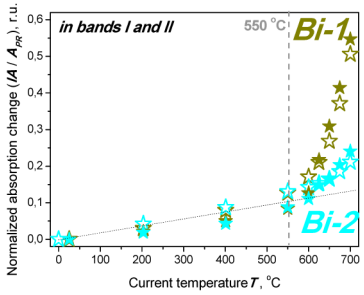

Fig. 15. Dependences of relative (as compared to pristine state, A_{PR}) absorption, IA/A_{PR}, established in Bi-1 (olive symbols) and Bi-2 (blue symbols) fibers versus current temperature T, at heating from RT to 700°C, measured in resonant-absorption bands I (open symbols) and II (filled symbols). Lengths of Bi-1 and Bi-2 fiber samples were 6 and 2 cm, respectively. The dashed and dotted-dashed lines show the characteristic essences obeyed by the dependences.

#251792 Received 12 Oct 2015; revised 27 Nov 2015; accepted 18 Dec 2015; published 15 Jan 2016

A similar difference between Bi-1 and Bi-2 fibers can be revealed from Fig. 15, where we compare susceptibilities of these two fibers to temperatures during heating, termed as IA/A_{PR} versus ***T***, in bands I and II.

First, it is seen from Fig. 15 the presence of already noticed two stages of IA-rise with ***T***. The first stage can be addressed as a weak and comparable for two fibers increase of IA (probably, related to small changes in absorption cross-sections and energy levels' lifetimes of BACs). In turn, at the second stage IA dramatically grows starting from ***T*** = 550°C, which, in our belief, is connected with an increase of concentration of BACs, responsible for resonant absorption. This phenomenon can be linked to some internal effects, given by the presence and specific properties against temperature of Bi and Bi-related specie in core-glass.

Second, ***T***-impact on establishing extra absorption (IA) in these two fibers, mainly differing in doping degree with Bi, is weaker in the heavier doped Bi-2 fiber than in Bi-1 one. That is, IA/A_{PR} in bands I and II is ~0.25 in Bi-2 fiber, whereas in Bi-1 this ratio exceeds 0.5.

In Fig. 16, we demonstrate how NIR fluorescence of BACs in Bi-2 fiber depends on current temperature ***T*** at heating from RT to 700°C (***T***-values label the spectra) and also as a result of 1-h. annealing at ***T**** = 700°C. The measurements were proceeded at P_P = 4.5 mW, in "forward geometry".

As seen from Fig. 16, elevating temperature resulted, at lower ***T*** (up to 400…500°C), in noticeable rise of Bi-related NIR fluorescence, which at higher temperatures (***T*** = 500…700°C) saturates in magnitude but continues to suffer broadening. That is, behavior of NIR fluorescence with increasing ***T*** was somewhat different in Bi-2 fiber as compared to Bi-1 one (compare Figs. 16 and 8). In the meantime, annealing Bi-2 sample at high temperature for 1 h. (compare the two violet spectra in Fig. 16, obtained at the highest temperature, ***T*** = 700°C) led to small but detectable extra-rise of NIR fluorescence. Furthermore, cooling of annealed Bi-2 fiber to RT resulted in NIR fluorescence rise, as compared with its pristine state, which is schematized in Fig. 16 by the red vertical arrow. This shows that an increase of concentration of fluorescing BACs takes place in Bi-2 fiber as the result of annealing at high (>550°C) temperature. These two details are similar to what was noticed for Bi-1 fiber. As well, spectral shifting with ***T*** of NIR fluorescence peak towards shorter wavelengths, is seen to apply for Bi-2 fiber, too.

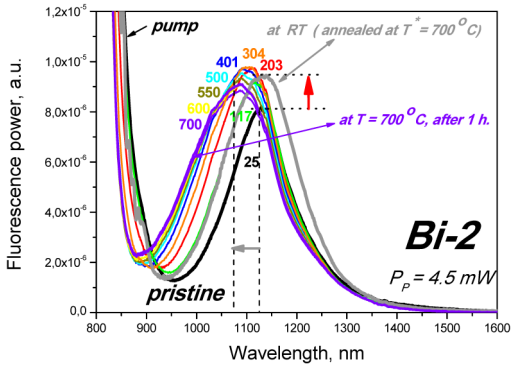

Fig. 16. NIR fluorescence spectra of Bi-2 fiber measured at different temperatures ***T*** (labeled near each curve) at heating from RT to 700°C, in "forward geometry". The black spectrum corresponds to pristine fiber while the two violet spectra – to ***T*** = 700°C just after establishing this temperature and after 1 h. of annealing. The grey spectrum, measured at RT, corresponds to the case when Bi-2 sample has passed a whole cycle of heating to 700°C, annealing during 2 h. at this temperature, cooling to RT, and thermal relaxation for 24 h. (i.e. ***T**** = 700°C). The arrows guide to the eye the most appreciable trends that NIR fluorescence obeys during thermal treatment. Pump power at 750 nm was fixed at P_P = 4.5 mW.

#251792 Received 12 Oct 2015; revised 27 Nov 2015; accepted 18 Dec 2015; published 15 Jan 2016

The reported details are better seen from Fig. 17 where overall "dynamics" of (a) NIR fluorescence power peaking at ~1.15 μm and (b) of pump saturating the NIR fluorescence, P_P^{sat}, against temperature is demonstrated (the notations in Fig. 17 are the same as in Fig. 9).

From Fig. 17(a), it is seen that, on the contrary to what happens with Bi-1 fiber (a very big, >4 times, increase of NIR fluorescence power as the result of annealing at $\boldsymbol{T}$ = 700°C: refer to Fig. 9(a)), this effect in Bi-2 fiber is less pronounced (~30%, see the grey vertical arrow, highlighting the said). However, annealing Bi-2 fiber at lower than 550°C temperature did not result in irreversibility in fluorescent ability, on the contrary to Bi-1 fiber's case.

On the other hand, see Fig. 17(b) and compare it with Fig. 9(b), the dependences $P_P^{sat}(\boldsymbol{T})$ for both (Bi-2 and Bi-1) fibers look similarly, differing in details only. The first difference is that P_P^{sat} grows with $\boldsymbol{T}$ in case of Bi-1 fiber with bigger slope and accesses bigger values at higher $\boldsymbol{T}$ than in case of Bi-2 fiber. The second difference is that the two stages in the $P_P^{sat}(\boldsymbol{T})$ dependence, clearly seen in Fig. 9(b), for Bi-1, are less expressed than in Fig. 17(b), for Bi-2.

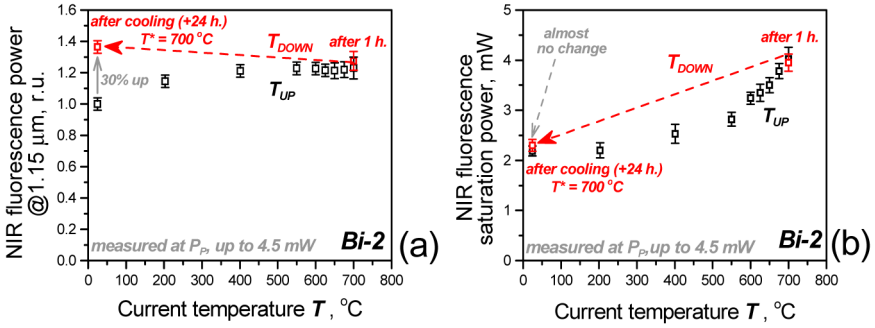

Fig. 17. Dependences of (a) integrated NIR fluorescence power and (b) pump power saturating 1.15-μm fluorescence versus temperature $\boldsymbol{T}$, for Bi-2 fiber. Specified are the processes of heating (T_{UP}: black symbols), 1-h. annealing at $\boldsymbol{T}$ = 700°C (right-hand red symbols), and posterior cooling to RT and thermal relaxation during 24 h. (i.e. $\boldsymbol{T}^*$ = 700°C) (T_{DOWN}: left-hand red symbols). Pump power at 750 nm P_P was varied at measurements of NIR fluorescence saturation (b) from a few μW to 4.5 mW.

The data obtained at testing Bi-2 fiber from the viewpoint of fluorescence lifetime dependences, at 750-nm pumping, on temperature are not shown here as they were found to be similar to the ones shown in Fig. 12 for Bi-1 fiber. The reader is advised here to refer to [16] where Bi-1 and Bi-2 fibers were studied, in this sense, for the temperature interval ranged from RT up to 500°C, where an insignificant difference in lifetimes of NIR fluorescence between the two fibers is demonstrated, being the effect of UC (a bit stronger expressed in Bi-2 fiber). Furthermore, note that almost no deviations in the fluorescence lifetimes' behavior against temperature for Bi-1/Bi-2 fibers were detected for $\boldsymbol{T}$ ranged between 500 and 700°C. We also omit here the most of the data obtained at testing optical response of Bi-2 fiber to heating using "backward geometry" (refer to Fig. 2(b)), again because of similarity of the main essences, found for both YAS-BDF fibers (highlighted and commented in Figs. 10 and 11, for Bi-1 fiber). Namely, the effects of weakening of VIS (centered at 820 nm) and simultaneous strengthening of NIR (centered at 1.15 μm) backward fluorescence, accompanied by dropping of pump-light backscattering (at 750 nm) at heating BDFs (T_{UP}), and partial restoring of these characteristics in the fibers after annealing at a high ($\boldsymbol{T}^*$>550°C) temperature (T_{DOWN}) were found to be equally pronounceable.

We only provide here, as an example (Fig. 18), comparison between 8-cm Bi-1 and 4-cm Bi-2 samples in terms of dependence of pump backscattering on temperature.

#251792 Received 12 Oct 2015; revised 27 Nov 2015; accepted 18 Dec 2015; published 15 Jan 2016

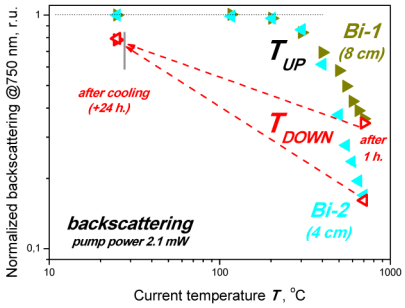

Fig. 18. Normalized dependences of backscattering at pump wavelength (750 nm) against temperature ***T***, obtained with Bi-1 (olive curve) and Bi-2 (blue curve) fibers, during heating (T_{UP}), after 1-h. annealing at ***T*** = 700°C (right-hand red symbols), and after annealing, cooling to RT, and thermal relaxation during 24 h. (i.e. ***T**** = 700°C) (T_{DOWN}: left-hand red symbols). Normalization was done to backscattering signals, measured using pristine Bi-1/Bi-2 fibers. Lengths of Bi-1 and Bi-2 fibers were 8 and 4 cm, respectively; pump power at 750 nm was fixed at P_P = 2.1 mW.

It is seen that decreasing of a backscattered signal at the pump wavelength (with respect to its value measured in the fibers' pristine states) is stronger in Bi-2 than in Bi-1 fiber. This detail is in agreement with IA-features, reported above for Bi-2 fiber in Fig. 13 and for Bi-1 fiber in Fig. 6 (see the blue spectra). Thus, we conclude that a decrease of scattering loss at heating is stronger in the heavier doped Bi-2 fiber than in the lower doped Bi-1 one, whilst an opposite trend is revealed if the fibers are compared in terms of IA (refer to Fig. 15). Seemingly, both phenomena are linked to re-structuration of core-glass in places where Bi related specie are located, as it is reasonable to bridge them to the presence of Bi in the fibers.

Some arguments in favor the last hypothesis are given by the data of Raman analysis of YAS-BDFs: see the next Section.

4. Additional notes

4.1. Raman-scattering studies of Bi-1 and Bi-2 BDFs and discussion

The experimental arrangement employed at making Raman analysis of the YAS-BDFs is described in [17]; let us only note that the excitation wavelength was 514.5 nm (Argon laser) and that BDF samples under study were 20…30-cm in length, being in pristine (before thermal treatment) or annealed (***T**** = 700°C) states. Specifically, the black and grey spectra in Fig. 19 (see below) were measured at handling the pristine and annealed samples, at RT. All spectra presented in Fig. 19 were obtained after normalization of the original experimental ones on maxima, located at ~450…500 cm^{-1} (adherent to the main SiO_2 vibration mode); thus, their direct comparison is worth of making. This procedure does not lead to loosing information or its serious distortion, especially if one seeks differences in details within a spectrally limited range (as done below).

It is seen from Fig. 19 that notable changes in the Raman-scattering signals are produced within the spectral range 30…220 cm^{-1}, known [19–22] as the region where the features, most relevant to doping silica-glass with Bi, are present. Growth of Raman components in this interval after annealing both fibers (compare curves 1 and 2 in panels (a) and (b) and their zooms) signifies a serious perturbation (re-structuration) of the local core-glass network, enriched with Bi (which can be nanocluster inclusions of Bi_2O_3-SiO_2 glass; see below).

#251792 Received 12 Oct 2015; revised 27 Nov 2015; accepted 18 Dec 2015; published 15 Jan 2016

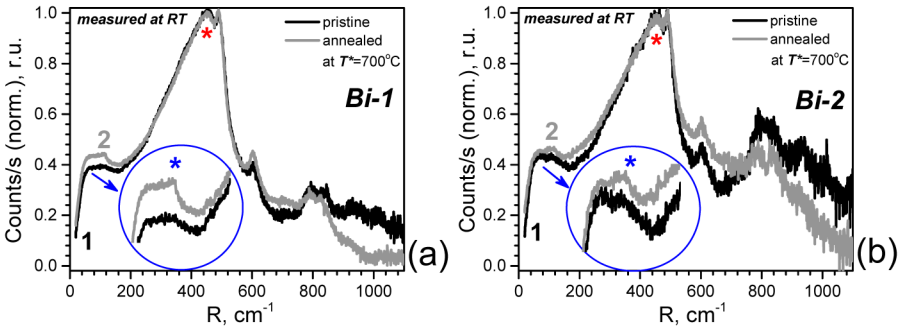

Fig. 19. Experimental (normalized on the peak's value, see red asterisk) Raman spectra of (a) Bi-1 and (b) Bi-2 fibers, obtained before thermal treatment (black curves 1) and after annealing at T^* = 700°C (grey curves 2). Insets demonstrate zooms of the spectra, for the range 30…220 cm^{-1} (see images inside the blue circles and blue asterisks).

A type of the changes that would suffer sub-networks of the core-glass enriched in Bi cannot be reliably determined from this result. Nonetheless, it can be proposed that such complexes as lower-valence Bi-forms (possibly joined by covalent bonds, or capturing defects from nearby: see below) were excessively, relating to the pristine state, formed as the result of high-temperature annealing. Among the low-valence Bi-forms, the interstitial Bi_0, Bi^-, and Bi_2^- centers (with possible defects in close vicinity), or oxygen-deficient centers of = Bi…Bi = and = Bi…Si≡ types should be proposed, all generating pronounceable Raman signals within the spectral area, zoomed in Fig. 19 [19–21]. Noteworthy, some of such Bi-related specie seem to be candidates for NIR fluorescence in a 1.0…1.2-μm range. Therefore, rise of the Raman signal's magnitude within the 30…220 cm^{-1} range, detected for both Bi-1 and Bi-2 fibers, is an argument in support of the idea that extra fluorescence-active BACs are "generated" in the fibers during heating and/or after high-temperature annealing. In our belief, it is a reasonable hypothesis as it correlates with the experimental observations made in Section 3, i.e. with growth of BACs resonant-absorption bands and NIR (1.15-μm) fluorescence, arisen after high-temperature treatment of the fibers.

Another feature that can be captured from the Raman spectra in Fig. 19 is that they demonstrate overall depression in magnitude, for both fibers, as the result of annealing (this is well seen at bigger wavenumbers – compare curves 1 and 2). We can propose that this feature is related to decreasing of the 750-nm scattered signal, measured in the "backward geometry", when compared are the pristine and annealed states of Bi-1/Bi-2 fibers (refer to Fig. 18).

4.2. Hypotheses about physical mechanisms underlying the thermally induced effects in BDFs

To the end, we present synopsis of the ideas based on the literature data, adherent to above discussed matters, in attempt to seek possible mechanisms, underlying the temperature-related effects in the YAS-BDFs.

First, notice that the EDX-analysis of the Bi-doped nano-engineered YAS-based preforms, sourcing Bi-1 and Bi-2 fibers, has shown [17] a phase separation of the core-glass, being dispersing of abundant in Bi clusters (a few nm in size), surrounded by almost Bi-free host. It is worth proposing that Bi-rich clusters are a kind of binary SiO_2–Bi_2O_3 (bismuthate-silicate) glass with a relatively high content of Bi_2O_3 phase inside YAS glass, weakly doped with Bi. Furthermore, given that the ED analysis of the preforms has demonstrated absence of any crystallinity in their cores, the presence of crystal-like Bi-rich chains – such as $Bi_{12}SiO_{20}$, $Bi_4Si_3O_{12}$, or Bi_2SiO_5 – was almost improbable at the preform stage. Furthermore, though the EDX analysis of the final Bi-1/Bi-2 fibers was incapable to resolve such phase separation after drawing the fibers from the preforms [17], the presence of nano- (or sub-nano) structuration of the core glass (*viz*. SiO_2–Bi_2O_3 clusters) at the fiber stage can be assumed (the

#251792 Received 12 Oct 2015; revised 27 Nov 2015; accepted 18 Dec 2015; published 15 Jan 2016

Raman analysis presented in [17] gave evidences for that). The presence of abundant in Bi inclusions (i.e. nano-clusters of bismuthate-silicate glass) in our YAS-BDFs can be, from one side, a cause of the thermally induced effects, reported above, and, from the other side, a factor explaining differences in appearance of these effects in our case and in case of Ref [15]. [In [15], D. Dvoretskii *et al*. reported, for alumino-silicate fiber low-doped with Bi, similar effects, i.e. rise of the resonant-absorption bands of BACs and enhancement of NIR fluorescence after annealing, which however were found to arise at temperatures above 1100°C.] Thus, the facts of relatively high (our YAS-BDFs) and of extremely low (non-resolved) [15] doping with Bi are meaningful for understanding differences in the thermally induced effects in BDFs of these two types.

An explanation of the main finding of the present study (a dramatic increase of BACs resonant-absorption bands and pronounceable growth of NIR fluorescence in Bi-1/Bi-2 fibers during and after heating) is – according to our current view – "generation" of extra BACs as a result of the high-temperature treatment. In turn, a general cause of producing extra BACs in the fibers at a high temperature can be the reduction-type reaction $Bi^{3+}\rightarrow Bi^{2+}\rightarrow Bi^{+}\rightarrow Bi^{0}$ at increased temperature, well-documented for binary bismuthate-silicate glasses and guessed for Bi doped alumino-silicate glasses (see e.g [15,23–27].). Note that, in pristine BDFs, SiO_2–Bi_2O_3 clusters may be the areas where the referred above reaction goes, since Bi should have 3^{+}-valence there. In turn, producing in a BDF, via heating and annealing, of lower than 3^{+}-valent Bi ions "opens" a channel for creating such specie as e.g. Bi_2^{-} defected centers and oxygen-deficient = Bi…Bi = and = Bi…Si≡ ones, supposedly fluorescent-active in NIR (see above).

Furthermore, the presence (in the majority of the experimental dependences reported above for Bi-1/Bi-2 fibers) of the stage, beginning at temperatures above 550°C – at which all the changes suffered by the fibers become drastic – also deserves a comment. We think that the key point in this sense would be possible presence of SiO_2–Bi_2O_3 nano-clusters in pristine fibers. According to the literature data (see e.g., Refs [28,29].), the dissociation reaction $2Bi_2O_3\rightarrow 4Bi + 3O_2$ gets started at heating a glass sample doped with Bi_2O_3 up to 550…700°C. The result of this can be effective deliberating of Bi-atoms and accelerating mobility of O-atoms in the host glass, at temperatures higher than 500°C. The mentioned dissociation reaction concretizes the meaning of the reduction sequence referred to above ($Bi^{3+}\rightarrow Bi^{2+}\rightarrow Bi^{+}\rightarrow Bi^{0}$), capable of producing extra BACs at high temperature. Thus, the presence of stage "2" in the most of the dependences reported above, "switched" once $\boldsymbol{T}/\boldsymbol{T}^{*}$ overcomes 500°C, becomes understandable. Moreover, re-structuration of the core-glass of Bi-1/Bi-2 fibers in areas enriched with SiO_2–Bi_2O_3 nano-clusters (in pristine state) can have other consequences of dissociation. One of them can be "homogenization" of core-glass owing to Bi_2O_3-clusters fading, with a probable result being a decrease of scattering loss (see Fig. 18). In this sense, it deserves attention that in binary bismuthate-silicate glass, at temperatures around 500°C, such critical points as glass transition, melting, and solidification are passed (see e.g. Refs [23,30–33].).

The difference between Bi-1 and Bi-2 fibers in susceptibility to thermal treatment, i.e. less pronounced high-temperature-induced effects in the heavier doped (Bi-2) fiber than in the lower doped (Bi-1) one, are unclear at the moment. We can only propose regarding this observation that, at very high Bi-doping, a potential of core-glass for sourcing defects at heating (see above), required for creating fluorescing BACs, is limited. This would lead, in the conditions of a high initial content of BACs (the case of Bi-2 fiber), to depleted effectivity of the dissociation reaction $2Bi_2O_3\rightarrow 4Bi + 3O_2$ and even to start of a reversed reaction. Another thing to say in this sense is that, expectedly, at a high Bi concentration, larger in size Bi-clusters can be formed in BDF core-glass, which would also stand behind a less-expressed effect of temperature on enhancing the fiber's absorptive/emissive properties; moreover, at the extremes, the formation of such clusters may even worsen them.

#251792 Received 12 Oct 2015; revised 27 Nov 2015; accepted 18 Dec 2015; published 15 Jan 2016

In the context of the discussion above, there should be referred the recent studies on thermal dependence of NIR fluorescence in Bi-doped glasses [34,35], where the changes happening with BACs at thermal treatment are inspected [34] and strong volatility and re-distribution of Bi and Bi-related BACs at thermal annealing of such glasses with different precursors is revealed [35]. Also note that similar effects of enlarging extinction in the resonant-absorption bands of Bi-Al related BACs and enhancing NIR fluorescence produced were recently reported, for alumino-silicate fibers, as resulted from other-type external influences, such as UV and electron irradiation and H_2-loading [36,37]. Finally, the recent overview [38] of the current problematics relating the physics of BACs in different glass hosts should be referred, where the current view on the matter is given and where, particularly, the issues relating to effect of high temperatures are addressed. It deserves mentioning that the hypotheses proposed by us above in attempt to explain phenomenology of the temperature-related effects in the YAS-BDFs do not contradict the ideas of Ref [38].

5. Conclusions

In this work, the effect of high (varied up to 700°C) temperature upon transformations of attenuation and fluorescence (at 750-nm excitation) spectra and upon variations of such parameters as fluorescence and resonant-absorption saturation, fluorescence lifetime, and pump-light scattering in a couple of yttria-alumino-silicate fibers heavily doped with Bi (YAS-BDFs) is studied. The whole of the collected dependences reveals, for both fibers, dramatic changes in these characteristics at temperature overcoming "threshold" being 500…550°C. At heating the fibers above this temperature, rise of resonant absorption in all bands of Bi-related "active" centers (BACs) and BACs fluorescence in NIR (peaked at ~1.15 μm) becomes tremendous. On the other hand, fluorescence, peaked at ~820 nm, rapidly weakens at heating the fibers from RT to 500…550°C, completely fading at overcoming this temperature. Furthermore, after high-temperature annealing of the fibers (at temperatures exceeding 500…550°C) growth of absorption in all bands of BACs and enhancement of the NIR fluorescence is "frozen" (*viz.* when measured at RT), thus manifesting considerable improvement of "state-of-the art" of the fibers as the ultimate result of high-temperature treatment. On the other hand, the fibers' microscopic parameters, such as BACs fluorescence lifetime and saturation power, though suffering considerable changes during heating, are preserved almost unchanged in their post-annealed state, as compared to pristine one. In virtue of these experimental laws, it is worth concluding that extra fluorescing in NIR BACs are "generated" in the fibers during heating and, what is more important for practical applications, as the result of high-temperature annealing. To our current understanding, the revealed phenomena are related to high doping with Bi of both the fibers under study and, thus, to the presence in their core-glass of Bi_2O_3 nano-clusters. According to the results of a comparative Raman analysis made with the BDFs being in pristine and annealed states and to the available literature data on high-temperature related phenomena in Bi_2O_3-rich silicate glass and fiber (our YAS-BDFs fibers certainly belong to this type of fiber), we hypothesize that the redox transformations in the fibers' core-glass underlie the high-temperature transformations, highlighted above. However, a more comprehensive study on the matter is certainly required to accept or reject this hypothesis.

Acknowledgments

This work was partially supported by the CONACyT (Project 242221, Mexico) and RFBR (Project 15-52-45024, Russian Federation). A. Kir'yanov kindly acknowledges financial support for temporal stay at the "MISiS" University through the Increase Competitiveness Program of NUST of "MISiS" of the Ministry of Education and Science of the Russian Federation (Project K3-2015-056, Russian Federation). A. Halder is thankful to the CSIR (India) for awarding a senior research fellowship.

#251792 Received 12 Oct 2015; revised 27 Nov 2015; accepted 18 Dec 2015; published 15 Jan 2016